2nd German Robotics Conference (GRC), Cologne, Germany, 2026.

MuST-C: The Multi-Sensor, Multi-Temporal, and Multi-Crop dataset for In-Field Phenotyping and Monitoring

Yue Linn Chong[1,2], Julie Krämer[3], Erekle Chakhvashvili[3], Elias Marks[1,2], Felix Esser[1,2,*], Ansgar Dreier[2], Radu Alexandru Rosu[4], Kevin Warstat[3], Ralf Pude[6,7], Sven Behnke[4,5], Onno Muller[3], Uwe Rascher[3,6], Heiner Kuhlmann[1,2], Cyrill Stachniss[1,5], Jens Behley[1,2], Lasse Klingbeil[1,2]

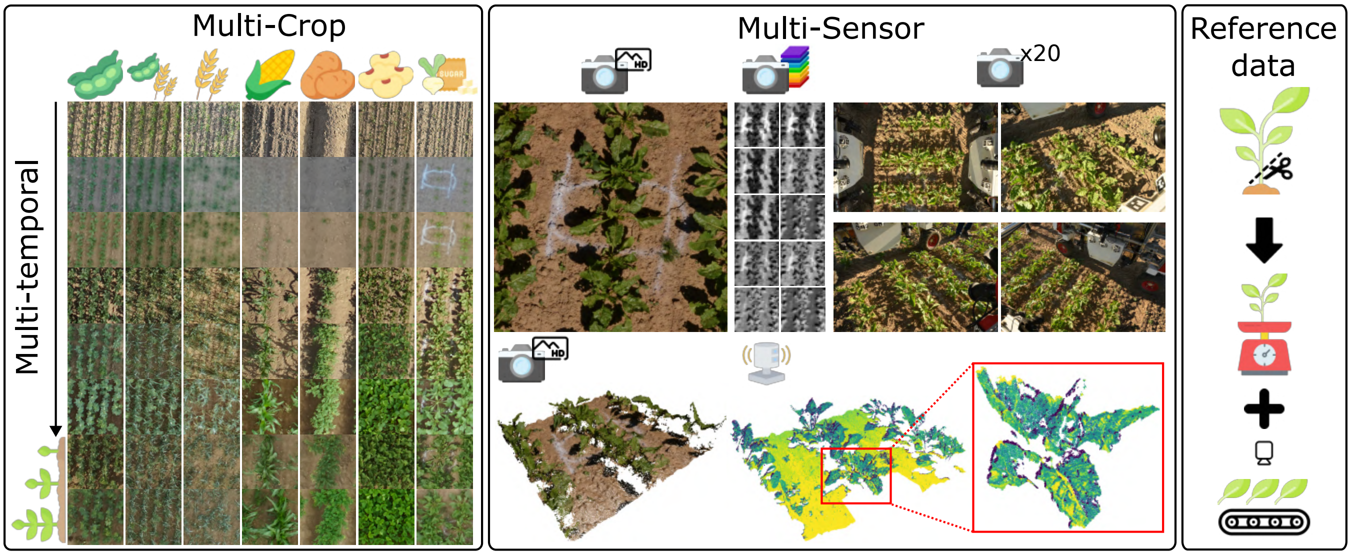

Fig. 1. Overview of our dataset, comprising a field trial with multiple crops, with sensor data collected at several time points. We collected data using multiple sensors; here, we showcase our georeferenced data, showing the same location in a sugar beet plot across multiple sensors in the middle section. From top left, we show the data from RGB orthophotos, multispectral orthophotos, four of the 20 RGB instantaneously captured images, a colored dense point cloud from RGB structure-from-motion, and the high-resolution LiDAR point cloud. With our georeferenced data, we can align data from different sensors and dates. In addition, we provide destructive reference measurements for aboveground fresh weight and LAI for the field trials. The MuST-C dataset is available via our project webpage `https://www.ipb.uni-bonn.de/data/MuST-C/` or directly via the bonndata public access repository `https://doi.org/10.60507/FK2/OX9XTM`.

Agricultural robots must meet the demands of a growing population while coping with climate change [1], [2]. Research and development of crop varieties that provide high yields and withstand climate impacts are crucial for increasing the efficiency of sustainable agricultural systems [3], [4] and require assessing phenotypic traits [5]. However, phenotyping remains a time-consuming and laborious task, often relying on manual, destructive measurements.

Moving towards automated high-throughput phenotyping is a key step to enhance the temporal frequency, repeatability, and objectiveness of measurements [6], [7]. The development of innovative methods, particularly those utilizing mobile sensing, depends on the availability of domain-specific data under real-world conditions. While agricultural field datasets exist [8], [9], they often represent a single growth stage, crop, or sensor type, limiting direct comparisons across sensor modalities, growth stages, or multiple crops. To address this, we introduce the multi-sensor, multi-temporal, multi-crop (MuST-C) dataset as presented in our original publication [10]. We collected data using diverse sensing modalities, including RGB cameras, multispectral cameras, and LiDAR sensors, mounted on robotic platforms (UAVs and UGVs). Georeferencing via GNSS receivers ensured data alignment across sensors and over time. For evaluation, we provide reference data for plant traits such as biomass and leaf area index (LAI), with LAI measurements validated through destructive methods.

Beyond LAI [11], [12] and biomass estimation [13], the MuST-C dataset supports various tasks, including crop-weed segmentation [14], plant counting [15], [14], leaf counting [16], [17], vegetation index retrieval, plant height estimation [18], and leaf angle distribution analysis. Further applications include plant reconstruction [19], plant density estimation [20], vegetation segmentation [21], and radiation use efficiency estimation [3]. Reflecting the growing interest in foundation models [22], [23], our dataset facilitates self-supervised pretraining for agricultural applications like weed semantic segmentation [7], disease detection [24], or 3D reconstruction [25]. The key novelty of MuST-C lies in providing aligned data from multiple sensors, enabling comparisons across modalities and supporting the development of novel sensor fusion approaches.

The field experiments were conducted during the 2023 growing season at the Campus Klein-Altendorf research facility of the University of Bonn, Germany. The study comprised six sub-experiments cultivated in 7.5 m × 6 m plots. These included five conventionally managed monocultures—sugar beet, spring wheat, sweet corn, soybean, and potato—and one organic wheat-faba bean intercrop trial. To simulate organic farming practices, no fertilizers or herbicides were applied in the wheat-faba bean trial. We compared 1:1 cereal-legume mixtures against monoculture controls in a two-block design. The mixtures combined the faba bean variety Fanfare with either short-growing (Anabel) or tall-growing (Sorbas) spring wheat, sown at half the density of the monocultures (monocrop reference densities: 320 seeds m^{-2} for wheat, 36 seeds m^{-2} for faba bean). Data were collected from the field experiment using various sensor modalities mounted on three different unmanned aerial vehicles (UAVs) and one unmanned ground vehicle (UGV). The specific sensors and collected data are detailed below.

UAV1 High-Resolution RGB Images (11664×8750 pixels) were captured in nadir view from UAV1. Flights were conducted at an altitude of 21 m, yielding a ground sampling distance of approximately 1 mm, with 70% side and 74% frontal overlap. Photogrammetric processing using Agisoft Metashape Pro, including structure from motion via bundle adjustment initialized with RTK poses and aligned using ground control points (GCPs), generated a point cloud and an orthophoto for each collection date.

UAV2 LiDAR Point Clouds carries a RIEGL miniVUX-SYS consisting of the RIEGL miniVUX-2UAV 2D laser scanner and the Applanix APX-20 inertial measurement unit. We configured the LiDAR sensor to the laser pulse repetition rate of 200 kHz and the scan speed of 53.80 lines per second. For georeferencing, we used a reference station to estimate the GNSS baseline and performed pose estimation with the inertial measurement unit (IMU) and additional GNSS data. We used the software RIEGL RiPROCESS for direct georeferencing, which combined the trajectory and LiDAR data. We filtered the LiDAR data by the maximum range of 45 m, and the resulting georeferenced point cloud has a mean density of 1433 pts m^{-2}.

UAV3 Multispectral Images are collected using a 10-band camera mounted on a Ronin MX gimbal, maintaining a nadir view. Images of the entire field trial were acquired with a ground sampling distance of 3 cm, utilizing a flight pattern with 90 % along-path and 65 % side overlap. Flights were planned under stable illumination conditions. Reflectance calibration for each orthophoto involved nine near-Lambertian calibration panels (2 % to 63 % reflectance) placed on bare soil. Raw multispectral images were processed to radiance units and georeferenced using GCPs and Agisoft Metashape Pro. Reflectance orthophotos were calibrated using the empirical line method. The dataset includes multispectral images, camera calibrations, and multispectral reflectance orthophotos for each collection date.

UAV3 RGB Images In conjunction with multispectral data, an RGB camera was mounted on the same gimbal on UAV3. These images were processed using Agisoft Metashape Pro to generate digital elevation models (DEMs) and orthophotos with an approximate ground sampling distance of 3 cm and estimated overlaps of 80 % along-path and 75 % to the sides. The dataset contains RGB images, camera calibrations, RGB orthophotos, and DEMs for each collection date.

UGV RGB Multi-Cameras The UGV was equipped with 20 RGB cameras (45.7MP, 8256×5504 px) positioned with adjustable zoom levels to maximize crop area coverage. The UGV traversed destructive sampling paths, acquiring images until canopy height became prohibitive. Camera zoom levels were manually calibrated daily based on crop canopy height. Camera intrinsic and scaled extrinsic parameters were calibrated using Agisoft Metashape Pro for each day. The data package provides sets of instantaneously captured 20 RGB images, organized by plot, and camera calibrations for each collection date.

UGV Point Clouds The UGV integrates two LMI laser triangulation scanners with overlapping fields of view and an Ouster OS1 64-beam LiDAR. Georeferencing involved the GNSS/IMU trajectory to the laser profiles in a global coordinate frame. System calibration (transformation between scanners and the INS) was performed using a 3D point feature approach. Sequences of point clouds from each LiDAR (left and right LMI, Ouster) were merged into larger point clouds, then cropped and organized by plot. Post-processing merged left and right LMI point clouds using a custom plane-to-plane iterative closest point algorithm to address potential misalignments (less than 10 cm) due to UGV deformation on uneven terrain. LMI point clouds offer higher density, enabling detailed distinction of single plant organs compared to Ouster data.

Author Affiliation

[1] Center for Robotics, University of Bonn, 53115 Bonn, Germany

[2] Institute of Geodesy and Geoinformation, University of Bonn, 53115 Bonn, Germany

[3] Institute of Bio- and Geosciences, IBG-2: Plant Sciences, Forschungszentrum Jülich GmbH, 52428 Jülich, Germany

[4] Department for Computer Science, University of Bonn, 53115 Bonn, Germany

[5] Lamarr Institute for Machine Learning and Artificial Intelligence, Germany

[6] Institute of Crop Science and Resource Conservation, Faculty of Agricultural, Nutritional and Engineering Sciences, University of Bonn, Germany

[7] Field Lab Campus Klein-Altendorf, Faculty of Agricultural, Nutritional and Engineering Sciences, University of Bonn, Germany

[*] Corresponding author: `esser@igg.uni-bonn.de`

Acknowledgment

This work has been partially funded by the German Research Foundation under Germany's Excellence Strategy, EXC-2070 - 390732324 – PhenoRob.

REFERENCES

[1] J. Schmidhuber and F. N. Tubiello, "Global food security under climate change," *Proceedings of the National Academy of Sciences*, vol. 104, no. 50, pp. 19703–19708, 2007.

[2] A. Wijerathna-Yapa and R. Pathirana, "Sustainable Agro-Food Systems for Addressing Climate Change and Food Security," *Agriculture*, vol. 12, no. 10, p. 1554, 2022.

[3] M. Reynolds, S. Chapman, L. Crespo-Herrera, G. Molero, S. Mondal, D. N. Pequeno, F. Pinto, F. J. Pinera-Chavez, J. Poland, C. Rivera-Amado, C. Saint Pierre, and S. Sukumaran, "Breeder friendly phenotyping," *Plant Science*, vol. 295, p. 110396, 2020.

[4] M. Watt, F. Fiorani, B. Usadel, U. Rascher, O. Muller, and U. Schurr, "Phenotyping: New Windows into the Plant for Breeders," *Annual Review of Plant Biology*, vol. 71, pp. 689–712, 2020.

[5] J. L. Araus and J. E. Cairns, "Field high-throughput phenotyping: the new crop breeding frontier," *Trends Plant Sci.*, vol. 19, no. 1, pp. 52–61, 2014.

[6] E. Marks, J. Bömer, F. Magistri, A. Sah, J. Behley, and C. Stachniss, "BonnBeetClouds3D: A Dataset Towards Point Cloud-Based Organ-Level Phenotyping of Sugar Beet Plants Under Real Field Conditions," in *Proc. of the IEEE/RSJ Intl. Conf. on Intelligent Robots and Systems (IROS)*, 2024.

[7] J. Weyler, F. Magistri, E. Marks, Y. L. Chong, M. Sodano, G. Roggiolani, N. Chebrolu, C. Stachniss, and J. Behley, "PhenoBench — A Large Dataset and Benchmarks for Semantic Image Interpretation in the Agricultural Domain," *IEEE Trans. on Pattern Analysis and Machine Intelligence (T-PAMI)*, vol. 46, no. 12, pp. 9583–9594, 2024.

[8] L. Roth, H. Aasen, A. Walter, and F. Liebisch, "Extracting leaf area index using viewing geometry effects—A new perspective on high-resolution unmanned aerial system photography," *ISPRS Journal of Photogrammetry and Remote Sensing*, vol. 141, pp. 161–175, 2018.

[9] R. Raj, J. P. Walker, R. Pingale, R. Nandan, B. Naik, and A. Jagarlapudi, "Leaf area index estimation using top-of-canopy airborne RGB images," *International Journal of Applied Earth Observation and Geoinformation*, vol. 96, p. 102282, 2021.

[10] Y. L. Chong, J. Krämer, E. Chakhvashvili, E. Marks, F. Esser, A. Dreier, R. A. Rosu, K. Warstat, R. Pude, S. Behnke, *et al.*, "The multi-sensor and multi-temporal dataset of multiple crops for in-field phenotyping and monitoring," *Scientific Data*, 2026.

[11] E. Chakhvashvili, J. Bendig, B. Siegmann, O. Muller, J. Verrelst, and U. Roscher, "LAI and Leaf Chlorophyll Content Retrieval Under Changing Spatial Scale Using a UAV-Mounted Multispectral Camera," in *Proc. of the IEEE Intl. Geoscience and Remote Sens. Symposium (IGARSS)*, 2022.

[12] S. Shafian, N. Rajan, R. Schnell, M. Bagavathiannan, J. Valasek, Y. Shi, and J. Olsenholler, "Unmanned aerial systems-based remote sensing for monitoring sorghum growth and development," *PLoS One*, vol. 13, pp. 1–15, 05 2018.

[13] D. M. Deery, G. J. Rebetzke, J. A. Jimenez-Berni, A. G. Condon, D. J. Smith, K. M. Bechaz, and W. D. Bovill, "Ground-Based LiDAR Improves Phenotypic Repeatability of Above-Ground Biomass and Crop Growth Rate in Wheat," *Plant Phenomics*, vol. 2020, p. 8329798, 2020.

[14] J. Weyler, T. Läbe, J. Behley, and C. Stachniss, "Panoptic Segmentation with Partial Annotations for Agricultural Robots," *IEEE Robotics and Automation Letters (RA-L)*, vol. 9, no. 2, pp. 1660–1667, 2024.

[15] Y. Fang, X. Qiu, T. Guo, Y. Wang, T. Cheng, Y. Zhu, Q. Chen, W. Cao, X. Yao, Q. Niu, *et al.*, "An automatic method for counting wheat tiller number in the field with terrestrial LiDAR," *Plant Methods*, vol. 16, p. 132, 2020.

[16] G. Roggiolani, M. Sodano, F. Magistri, T. Guadagnino, J. Behley, and C. Stachniss, "Hierarchical Approach for Joint Semantic, Plant Instance, and Leaf Instance Segmentation in the Agricultural Domain," in *Proc. of the IEEE Intl. Conf. on Robotics & Automation (ICRA)*, 2023.

[17] J. Weyler, F. Magistri, P. Seitz, J. Behley, and C. Stachniss, "In-Field Phenotyping Based on Crop Leaf and Plant Instance Segmentation," in *Proc. of the IEEE Winter Conf. on Applications of Computer Vision (WACV)*, 2022.

[18] A. Dreier, G. Lopez, R. Bajracharya, H. Kuhlmann, and L. Klingbeil, "Structural wheat trait estimation using uav-based laser scanning data: Analysis of critical aspects and recommendations based on a case study," *Precision Agriculture*, vol. 26, no. 1, p. 18, 2025.

[19] E. Marks, F. Magistri, and C. Stachniss, "Precise 3D Reconstruction of Plants from UAV Imagery Combining Bundle Adjustment and Template Matching," in *Proc. of the IEEE Intl. Conf. on Robotics & Automation (ICRA)*, 2022.

[20] N. Wilke, B. Siegmann, J. A. Postma, O. Muller, V. Krieger, R. Pude, and U. Rascher, "Assessment of plant density for barley and wheat using uav multispectral imagery for high-throughput field phenotyping," *Computers and Electronics in Agriculture*, vol. 189, p. 106380, 2021.

[21] E. Marks, M. Sodano, F. Magistri, L. Wiesmann, D. Desai, R. Marcuzzi, J. Behley, and C. Stachniss, "High Precision Leaf Instance Segmentation in Point Clouds Obtained Under Real Field Conditions," *IEEE Robotics and Automation Letters (RA-L)*, vol. 8, no. 8, pp. 4791–4798, 2023.

[22] J. Gu, S. Stevens, E. G. Campolongo, M. J. Thompson, N. Zhang, J. Wu, A. Kopanev, Z. Mai, A. E. White, J. Balhoff, W. Dahdul, D. Rubenstein, H. Lapp, T. Berger-Wolf, W.-L. Chao, and Y. Su, "Bioclip 2: Emergent properties from scaling hierarchical contrastive learning," vol. arXiv:2505.23883, 2025.

[23] C.-H. Yang, B. Feuer, Z. Jubery, Z. K. Deng, A. Nakkab, Z. Hasan, S. Chiranjeevi, K. Marshall, N. Baishnab, A. K. Singh, A. Singh, S. Sarkar, N. Merchant, C. Hegde, and B. Ganapathysubramanian, "BioTrove: A Large Curated Image Dataset Enabling AI for Biodiversity," in *Proc. of the Conf. on Neural Information Processing Systems (NeurIPS)*, 2024.

[24] A. Benfenati, P. Causin, R. Oberti, and G. Stefanello, "Unsupervised deep learning techniques for automatic detection of plant diseases: reducing the need of manual labelling of plant images," *Journal of Mathematics in Industry*, vol. 13, no. 1, p. 5, 2023.

[25] D. Zermas, V. Morellas, D. Mulla, and N. Papanikolopoulos, "Estimating the Leaf Area Index of Crops Through the Evaluation of 3D Models," in *Proc. of the IEEE/RSJ Intl. Conf. on Intelligent Robots and Systems (IROS)*, 2017.